Journal of Mathematical Chemistry
https://doi.org/10.1007/s10910-024-01626-4

REVIEW

A review on recent theoretical approaches made in the discovery of potential Covid-19 therapeutics

Apurba K Bhattacharjee[1]

Received: 4 August 2023 / Accepted: 12 May 2024

Abstract

SARS CoV-2 virus (COVID-19) emerged as a highly infectious human pathogen in late 2019. Started in China but rapidly started spreading all over the world and soon became a pandemic. More than seven million deaths have been reported so far that devasted millions of families worldwide. Several drugs, such as hydroxychloroquine, chloroquine, remdesivir, favipiravir and arbidol have undergone some clinical studies since early 2020, but their safety concerns remained a serious issue. However, within an year from late 2019, several successful vaccines were invented to prevent people from the infection. Almost at the same time, two drugs were discovered. These are PAXLOVID™ (nirmatrelvir, ritonavir) from Pfizer and molnupiravir from Merck which were soon approved by the US-FDA, for emergency use in the treatment of COVID-19. But several challenges were soon reported in treatments with these drugs, particularly for those who are immunocompromised or have vaccine immunity and suffering for a long time from the infection (known as long-COVID). Complex issues for treatments of long-COVID patients continue to remain unresolved. Thus, discovery of new drugs to assist treatment for emerging COVID-19 problems is urgently needed. But it is important to note that discovery of new COVID-19 therapeutics, particularly small molecules is not a simple task. However, there are several excellent reviews on attempts for COVID-19 drug discovery including a handful of articles on theoretical approaches towards the goal. This review summarizes the theoretical attempts for discovery of COVID-19 drugs, their challenges and future opportunities along with efforts from the author's lab.

Keywords Covid-19 · Drug discovery · "Interaction pharmacophore" profiling · Molecular electrostatic potentials

✉ Apurba K Bhattacharjee
ab3094@georgetown.edu

[1] Biomedical Graduate Research Organization, Department of Microbiology and Immunology, School of Medicine, Georgetown University, Washington, DC 20057, USA

Published online: 28 May 2024

1 Introduction

Since the first outbreak of coronavirus, SARS-CoV-2 (COVID-19) in Wuhan province of China in late 2019, the virus started spreading all over the world at an unprecedented speed and soon emerged as perhaps the greatest medical tragedy of recent times [1]. WHO (World Health Organization) declared it a pandemic due it its virulence for infecting millions of people globally [2a]. Thus far, in addition to infecting millions of people worldwide, seven million people have died from the virus [2b]. Simultaneously, it created a huge impact on global societies demonstrating visible disparities in health care systems. It became a monumental task for most countries to tackle the urgently needed medical emergencies. Several mitigation efforts were advised by the WHO, such as country wide lockdowns, use of masks, repeated hand washings, and social distancing. Most of these mitigation efforts were implemented by most countries of the world at huge economic costs to save lives. However, during this critical period, a substantial investment was available for COVID-19 research in both life and allied sciences. The investment facilitated scientific responses ranging from innovations in viral characterization, new testing techniques, and sequencing of COVID-19. More important that research in this area enabled rapid publications of several valuable articles and papers to assist further COVID-19 research. These combined efforts led to the development of effective vaccines by many countries using variety of platforms at incredible speed. Several of these vaccines were approved by the WHO for prevention of COVID-19 [3], which undoubtedly saved millions of lives. However, global vaccination efforts had encountered several obstacles, such as lack of infrastructure for large scale vaccine manufacture, costs for manufacture, availability of trained personnel to immunize people, variability and durability of vaccine efficacy, vaccine hesitancy, and limitation of its efficacy in immunocompromised people [4]. Therefore, therapeutic interventions for COVID-19 infection were necessary. Discovery of potential therapeutics became an important goal for COVID-19 research. Although monoclonal antibody treatments were available for several months after the WHO pandemic declaration, with emergence of successive COVID-19 variants, these treatments became ineffective [5].

However, some anti-malarial drugs, such as hydroxychloroquine and chloroquine which were approved for treatment of autoimmune diseases were also widely reported to have potential benefit for prevention and treatment of COVID-19. But the Center for Disease Control (CDC) reported that the potential benefit of these drugs do not outweigh their risks in the prevention and treatment of COVID-19 [6]. Since hydroxychloroquine and chloroquine along with several other potential compounds were often debated to be included for clinical trials, clinical efficacy amongst large variations of patients remained unclear. But it is important to note that therapeutic discovery and development for COVOD-19 treatments is a complex, challenging and evolving problem due to virus mutations with newer mutants. Probably, that is why only two drugs, PAXLOVID™ (nirmatrelvir, ritonavir) from Pfizer and molnupiravir from Merck have so far obtained Emergency Use Authorization from the USFDA [7]. However despite initial success of PAXLOVID and molnupiravir, the drugs were found to have certain shortcomings, such as limited benefits for long term infections and eventual possibility for drug resistance [4, 8, 9]. Furthermore,

long COVID-19 is not only an emerging issue for the hospitalized patients but also for non-hospitalized patients, even with mild to moderate infection. More important, data indicate that patients admitted in hospitals with long COVID-19 having diabeties and cardiovascular diseases have higher risks of death compared to influenza patients. Long COVID-19 also appears to have neurological and cognitive issues along with multiple intellectual disabilities [9]. Long term effects of COVID-19 post-infection symptoms also have been reported to include the microbiota of the lungs and gut [10]. Pathogenic-profiles of gut–lungs microbiome interactions were implicated to affect the host immunity [10]. However, treatments became more difficult due to continuous evolution of the virus to adopt in the epithelial cells of lung and because the mechanism of long-COVID is still not well understood [11]. Despite the current sense of relief from the virulence of COVID-19 infection, approximately two hundred fifty thousand cases are reported every month globally [2b].

Thus, discovery of novel COVID-19 therapeutics is not only important and necessary but the choice of therapeutics should also include considerable attention to the above factors before selection for clinical trials. Several reviews on COVID-19 therapeutics were published [9, 11], however, only a handful were found that solely dealt with theoretical approaches for discovery attempts. In this review, recent theoretical attempts for discovery of COVID-19 therapeutics, their challenges and opportunities are discussed along with efforts made in the author's lab.

2 Summary discussions of recent published theoretical research on COVID-19 therapeutics

Thus to mention, Teixeira et al. [12] described an attractive drug target TMPRSS2 that was used for quantum and molecular mechanics calculations to understand the mechanistic path of acylation of proteolytic cleavage in the S protein at atomic levels. It is worthwhile to mention that the S protein (TMPRSS2) plays the most important role in the viral replication. The study was performed to provide an understanding for designing inhibitors of transition-state. The calculations helped to understand the mechanism of acylation and the proteolytic cleavage of the TMPRSS2 protein at atomic levels. The researchers found the acylation of TMPRSS2 to take place in two stages: (i) Ser441 to His296 proton transfer leading to a nucleophilic attack of Ser441 to the substrate's P1-Arg and (ii) His296 to the P1′-Ser residue proton transfer breaking the ArgP1-SerP1′ peptide bond. Activation energies were found to be 17.1 and 15.8 kcal/mol using Gibbs equation compared to the reactant. Overall results from the calculations indicated that TMPRSS2 interactions have limited scope for discovery of inhibitors without specific design in high-affinity analogues for TS inhibitors. However, the study supported a human target for development of more efficient COVID-19 drugs devoid of resistance in future [4, 8].

Teixeira et al. [12] and Bai et al. [13] further used density functional theory (DFT) at B3LYP and M06-2X levels and binding patterns to explore the free energy associated with cysteine proteases. Calculations were supported by the use of two other DFT methods (DFTB3 and GFN2-xTB) and two semi- empirical AM1d and PM6 methods. To regulate the activity of cysteine proteases development of inhibitors

are important which could eventually be potential drugs to counter many diseases, including COVID-19. Thus by using quantum chemical tools combining computational efficiency and accuracy, the authors explored the inhibition mechanism of the COVID-19- 3CL protease with a hydroxymethyl ketone derivative. The study further demonstrated that use of accurate and reliable computational strategy could provide reliable cost effective results efficiently. The strategy could also assist *in silico* screening targeting cysteine proteases for potential COVID 19 drug candidates [12–14].

Both theoretical and experimental aspects on remdesivir, the only drug that FDA approved for desperate situations in the treatment for COVOD-19 were dealt with by Li et al. [15]. However, the effectiveness of remdesivir is still under scrutiny by the WHO. But importantly, this article [15] described an alternative nucleoside, a metabolite (GS-441,524) of remdesivir to be a highly potent compound against COVID-19. This compound inhibited the replication of COVID-19 in Vero E6 cell lines. Furthermore, the authors tested it in both mouse model of COVID-19 and in mice infected with murine hepatitis virus (related to coronavirus) to show that the metabolite, GS-441,524 could be a promising cost effective drug candidate for treatment of COVID-19 [15].

Xu et al. [16] explored machine learning models to identify compounds capable of inhibiting the entry of COVID-19 into human host cells or the SARS-CoV-2 3-chymotrypsin-like (3CL) protease. This approach was described to be a better identification technique for compounds against COVID-19 than the traditional high-throughput (HTS) screening assays which have high costs but low hit rates. The authors concluded that optimizing the classification models, good results could be achieved and the models would be more cost effective and complementary to the HTS for screening compounds against COVID 19. Through this procedure, twenty-two compounds were identified and by experimental testing were found to have potent antiviral activities (<5 μM) against COVOD-19 in vivo virus assay.

Malla et al. [17] emphasized the role of the main protease (Mpro) as the target for discovery of COVID-19 drugs as well as for development for future treatments. The clinical efficacy of β-lactams as inhibitors for the bacterial nucleophilic enzymes led the authors to suggest that β-lactams could also be potential inhibitors for cysteine proteases and viral nucleophilic serine. Thus, the authors described a method for synthesis of derivatives of penicillin which could be potent inhibitors of Mpro and investigated the mechanism using mass spectrometric and crystallographic analyses. However, no theoretical transition state study was reported on the mechanism. Their results indicated the potential for activity of Mpro inhibitors through a nucleophilic cysteine formation through acyl−enzyme complex of β-lactams. Mechanism was further validated by crystallographic analysis. Finally, the authors demonstrated the importance of acylating agents for nucleophilic catalysis of β-lactams and the potential for inhibition of viral proteases [17].

Sasso et al. [18] in another article described the importance of RNA therapeutics and showed how RNA therapeutics have made a paradigm shift in clinical studies, research, and their commercial importance in physiological roles for medicines. Rapid development of lipid–RNA led to the development of nanoparticles for success of mRNA vaccines against COVID-19. Soon the focus led to research on discovery of RNA-based COVID-19 drugs and several such drugs were approved by FDA

for further clinical studies. The article detailed diverse functions of RNA covering the role of mRNA in antigen productions and protein therapeutics. The article also describes the regulatory roles of mRNA in tissues and cells. The authors concluded by highlighting the importance of RNAs as potential COVID-19 therapeutics, presented the current status and outlined the trends of the future for RNA research in medicines.

Vorobyov et al. [19] in a paper showed that differences perceived to be critical features through theoretical binding energy calculations of the two important spike proteins of SARS-CoV and SARS-CoV-2. The authors calculated the binding free energy of SARS-CoV-2 using a coarse-grained (CG) model for the human receptor ACE2. The free energy contributions were found to be from the residues located both outside the receptor binding domain as well as from the novel virus for a stronger binding. Two main conclusions from the binding calculations were: (a) evolution of SARS-CoV-2 happens remotely from the spike protein trimeric body at the domain level (b) Conformational changes are likely leading to the infection. Subsequently, the authors utilized their CG (coarse-grained) model for the free energy and binding energy calculations of each structure. The CG model had been used to specifically focus on electrostatic free energy of proteins. Additionally, solvation energy and charged - polar interactions were also calculated by the following equation:

$$\begin{aligned}&\mathbf{\Delta Gfold = \Delta Gmain + \Delta Gside + \Delta Gmain - side}\\&\mathbf{= c\,\Delta Gvdw + c\,\Delta GCG + c\,\Delta GCG + \Delta Gelec}\\&\mathbf{1\ side\ 2\ solv\ 3\ HB\ side}\\&\mathbf{+ \Delta Gpolar + \Delta Ghyd + \Delta Gelec + \Delta Gvdw}.\\&\mathbf{1\ side\ 2\ solv\ 3\ HB\ side}\\&\mathbf{+ \Delta Gpolar + \Delta Ghyd + \Delta Gelec + \Delta Gvdw}\end{aligned}$$

Free energy, ΔG-fold, comprising the above equations are: the main chain solvation energy, side chain van der Waals, hydrogen bond, electrostatic, side chain polar, side chain hydrophobic, main chain-side chain electrostatic, and main chain-side chain van der Waals energies, respectively. c1, c2, and c3 are the scaling coefficients which have values as 0.10, 0.25, and 0.15 in this work. Thus, from these calculations, a binding pattern between SARS-CoV antibody m396 and SARS-CoV-2 was established. From an absence of contribution of the remote energetics, the authors also suggested an absence of cross-reactivity between antibodies [19].

In addition, theoretical and experimental validation attempts for discovery of chemotherapeutics against COVID-19 infection were made by repurposing drugs from the existing antivirals, antimalarials, antibacterial, antiparasitic, immunosuppressants, anti-inflammatory and natural immune-stimulatory agents along with natural medicines [20, 21]. Dey et al. [20, 21] explored targets for SARS-CoV-2 (COVID-19) by docking-based screening of potential natural inhibitors. Furthermore, Nandi et al. [21] reported *in silico* structure-based docking studies by repurposing of US-FDA approved drugs. Biochemical mechanistic studies of repurposed drugs along with biological activity, pharmacokinetics and pharmacodynamic evaluations were also mentioned [21].

3 Summary discussions on theoretical approaches on COVID-19 therapeutics in the author's laboratory

Efforts made in the author's laboratory on the topic were presented and published earlier [22–24]. However, the study was further expanded and summarized here. It involved theoretical quantum chemical (QC) and empirical calculations on seven drugs (Chart I) frequently used at the initial stages for Covid-19 treatments [25–27]. The first objective was to develop an "interaction pharmacophore" model [24] from stereoelectronic properties and molecular electrostatic potential profiles of the above drugs. Next to utilize the model for search of databases to identify potential new anti-COVID-19 compounds. QC calculations on the above Covid-19 drugs provided a fairly accurate estimate of both stereoelectronic properties and "interaction-pharmacophore" profiles from molecular electrostatic potentials (MEPs) to enable development of a reliable model. The interaction pharmacophore model was compared with the interactions observed in the x-ray crystallographic structure of Covid-19 main protease 3CL-protease (MPro) and an inhibitor bound to it named X-77 [28]. After validating the similarity of interactions of X-77 with our developed model, a literature search for potential anti COVID-19 compounds was performed which resulted in identification isoquines and 4-aminoquinolines. Antiviral activities for three of the identified compounds, two aminoquinolines quinacrine (QC) & mefloquine (MQ) and an isoquine analog, N-tert-butyl isoquine were evaluated in assays used for antiviral potential of compounds, such as the replicon with expression of BHK-21 cell and infectivity plaques. Analysis of compounds in assays showed high antiviral activity for all three of them in the order N-tert-butyl isoquine > Mefloquine > Quinacrine and infectivity assay on them indicated a decreasing order of toxicity: N-tert-butyl isoquine < Mefloquine < Quinacrine thus the potential for anti-Covid-19 activity [23, 24]. Briefly, the study is described below.

Methodology adopted in the study is quantum chemical (QC) based computational calculations on all compounds presented in Chart I & II. Structure of compounds used for developing the model is shown in Chart I and compounds identified using the model are shown in Chart II. Lowest energy conformers with most abundancy in the gas phase state were selected for optimization of geometry of the compounds on which the electronic property calculations performed. However, geometry optimization and electronic energy calculations of compounds were sequentially performed starting from semi-empirical PM3 (Parameterized Model number 3) to density functional theory (DFT) with wB97X-D at 6-31G* level of basis set. The semi-empirical PM3 method generally provides optimized structures in accord with experimental structures since it is is based on the principle of Neglect of Differential Diatomic Overlap (NDDO) integral approximation in quantum mechanics. This also allows calculations suitable for polar surface area (PSA), because it is solely dependent on geometry. Molecular electrostatic potential (MEP) and three dimensional profiles were calculated and developed on the DFT-optimized structures of compounds using SPARTAN graphics [29]. MEP profiles were calculated on both van der Waals contact surface and beyond it so as provide an assessment of charge distribution viewed by an approaching molecule for interaction. Calculated energy range of MEP profiles beyond the van der Waals surface is approximately from − 80.0 to -20.0 kJ/mol

(–20.0 to −5.0 kcal/mol) which is usually recognized at a distance by the target protein molecule. MEP profiles on the van der Waals contact surface depicts a surface of constant electron density (0.002 e/au^3) onto which are superimposed electrostatic potentials with color-coding. These profiles not only provide the molecular size but also locations of most negative and most positive electrostatic potentials to assess the sites for interactions. Deepest red color location is the most negative electrostatic potential and thus the nucleophilic site, and the deepest blue color location is the most positive electrostatic potential and thus the electrophilic site. Therefore, these profiles are essentially the intrinsic reactivity profiles and known as "interaction pharmacophores" of molecules. Additionally, the calculated stereo-electronic properties also estimate dipole moments for electric field directions, molecular orbital energies for transition state assessments, and octanol/water partition coefficients (logP) for lipophilicity/hydrophobicity assessments of molecules.

In addition to MEP based interaction pharmacophores, chemical function descriptors (CFDs) were used to develop pharmacophores on the compounds to cross-validate the interactions of the model [24, 29]. Pharmacophore from CFDs provides locational assessments of (1) sterically-crowded region and aromatic π regions to determine hydrophobicity (2) aromaticity, (3) H-bond donor site for determination of acidic hydrogen atoms, (4) H-bond acceptor site for determination of lone pair positions, (5) positive ionizable site focusing the basic site, and (6) negative ionizable site focusing the acidic site of molecules. Excluded volumes for ligands can be estimated from structures extracted from PDB files. The CFD similarity analysis of molecules was performed on the basis of CFDs to get an insight of atom centric pharmacophore of molecules. The basis of similarity analysis is on molecules and/or pharmacophores [24. 29]. Different types of CFDs and their alignments and combinations are quantified by the following factorial equation:

i! j!k!. . . (where ! is the factorial symbol).

However, since calculation quickly turns unmanageable, limiting number of CFDs are used to represent the overall CFD pharmacophores [29].

Next, the x-ray crystallographic structure of COVID-19 (Protein Data Bank (https://www.rcsb.org/; PDB code: 6W63, 2.10 Å) [28] was used to develop a structure based pharmacophore. By downloading the three-dimensional coordinates of the main protease from the x-ray crystallographic structure with the bound inhibitor, X77, hydrogen atoms were added retaining water molecules in the protein structure. Then analysis of the protein- inhibitor complex was carried out and intermolecular interactions within 3 Å were determined to assess the structure-based pharmacophore.

In the discussion on the study results, it is to be noted that "interaction pharmacophore" was developed on all Chart I compounds except X-77. The Chart I compounds were all used for treatment of COVID-19 at the initial stage having varying successes [25–27]. X-77 is the ligand found as the inhibitor of 3CL-protease (Mpro) x-ray crystallographic structure [29] was used to validate the reliability of our interaction pharmacophore. Structure based determination for interactions of the inhibitor bound 3CL-protease (Mpro) crystallographic structure was found to be consistent with the possible interactions of our developed interaction pharmacophore model.

Stereoelectronic property results for both Chart I & II compounds indicate dipole moment directions towards the quinolone ring N atom and magnitude to be mostly

less than 6.0 debye units, log P (water/octanol partition coefficient) values to be less than 2.0 of and PSA (polar surface area) to be less than 50.0 A^2. In addition, Lipinsky empirical rule based the drug-likeness properties of the compounds also appear to be favorable [30 (a), (b)]. Furthermore, the compounds are not peptides and contain less than two carboxylic acid side chains in aromatic rings. Thus, the compounds should most likely be favorable for potential drug candidates (Chart I & II). In addition, calculations also support the drug likeness of the compounds from their favorable permeability, bioavailability, solubility, volume distribution, plasma protein binding, blood-brain barrier capacity and CNS crossing properties [31].

However, in order to obtain a deeper insight of intrinsic reactivity of the compounds (Chart I & II), profiles of molecular electrostatic potentials (MEP) were generated and analyzed. These profiles are well-known for recognition interactions since they carry key recognizable features to promote interaction with the target receptor at longer distances [32]. The profiles are essentially known as "interaction pharmacophores". It is a property that is created by the molecule's own nuclei and electrons as experienced by an approaching molecule in the surrounding space. Although it is an experimental property which can be determined by x-ray diffraction crystallography, it can also be accurately calculated using quantum chemical methods [32–34]. Mathematically, it is a measure of interaction capacity of a molecule imagined through interactions of a bare proton (H+) in close proximity of the molecular surface or van der Waals surface of a molecule.

Thus, MEP (r) at any point r^1 is the net result of the positive and negative contributions of the nuclei and electrons, where Z_α is the charge on nucleus α, located at R_α.

$$\mathbf{MEP(r)} = \sum_\alpha \mathbf{Z_\alpha/|r\text{-}R_\alpha|} - \int \boldsymbol{\rho}(\mathbf{r^1})\mathbf{dr^1}/\,|\mathbf{r\text{-}r^1}| \quad \ldots\ldots\ldots(1)$$

Since MEP provides an estimate of molecular charge distributions including the property of nucleus and electrostatic potential energy, therefore its nature can also be ascertained. Interactively, if a positive test probe is imagined to move along an atomic surface, the nucleus being positively charged a radially constant electric field will be experienced. Thus, a stronger positive charge that is a weaker negative charge would be experienced in the region of higher average electrostatic potential energy. Since the nuclei carry positive charges, higher potential energy value would indicate fewer electrons in this region and thus, absence of negative charges. Opposite would be case of atomic surfaces with electron rich regions. Molecular surfaces would also hold this property of electrostatics. Mathematically, charge distribution and electrostatic potential may be represented by the following equation:

Total Electrostatic Potential Energy $= \sum$**Electrostatic Potential Energy**

This equation is commonly used to find out electrostatic potentials. The total energy is calculated by addition of energies of a molecule interacting with every electric field produced along its surface.

MEP characterizes how a molecule is first encountered by an approaching molecule or a target protein. Therefore, the profile provides an insight of complex processes involving the dipole-dipole, charge-dipole and quadrupole-dipole interactions found in biological systems. MEP profile displays shape, size, charge distributions and reactive sites of a molecule simultaneously. The profiles also allow to visualize variable charged regions through varying gradation of colors of molecules (Figs. 1 and 2). Deepest red regions indicate most negative MEP regions characterized by

highest density of electrons, and therefore, the most nucleophilic site and most favorable for H-bond accepter (HBA) in the molecule. Deepest blue regions indicate most, positive MEP regions characterized by least electron density, and therefore, the most electrophilic site and most favorable for H-bond donor (HBD) in the molecule. Figures 1 and 2 (upper rows) show MEP profiles on van der Waals surface of compounds of Chart I & II compounds respectively.

The profiles of MEP beyond the molecular surface (van der Walls surface) are equally important for recognition interactions from a distance with the target receptor molecule. When MEP profiles are recognized by the target structure from a distance, it will promotes complementary interactions with the molecule. These profiles at approximately − 20.0 kcal/mol for Chart I & II compounds are shown in Figs. 1 and 2 (lower rows), respectively. A glance of Fig. 1 would indicate that the N atom of the quinoline ring in compounds 1 (CQ) and 2 (HCQ) (Chart I) has the most prominent negative potential profile whereas, compounds 3–6 have multiple negative potential regions. The specific feature of 1 & 2 indicates H-bond acceptor possibility of the N atom of the quinoline ring whereas, compounds 3–6 should have the possibility of multiple H-bond interactions. Probably the stronger hydrogen bond interaction of the quinoline N is linked to anti COVID-19 activity of both 1 & 2. Steric factors with the neighboring atoms probably hinder H-bond interactions of 1 (two more HBA) & 2 (three more) altogether. Dipole moment directions pointing towards the quinoline ring N atom in both 1 & 2 and consistency with the observed MEP profiles further strengthen the powerful nature of HBA character of the quinoline ring N atom of 1 & 2. Since compounds 3–8 show multipole directions of dipole moments and MEP locations, possibility of multiple weak hydrogen bonding interactions with the target molecule cannot be ruled out. However, for strong anti-COVID-19 activity, a stronger H-bond may be an important factor. Number of HBA and HBD counts of the of the compounds 3–8 perhaps also suggest weaker H-bonding capacity. Moreover, weak electrostatic potential distribution of large molecular surface (shades of green color), (Fig. 1 upper rows) would indicate a hydrophobic nature and therefore a possibility of hydrophobic interaction of the compounds with the receptor. Another interesting observation is the electrostatic potential region extending in one side of the molecules (Fig. 1 lower rows). This again indicates the region to be the most prominent and effective region for recognition with the target receptor. A strong role of hydrogen bonding and hydrophobic interactions are clearly apparent for complementary sites with the target protein which could be linked to anti-COVID-19 activity of Chart 1 compounds. Thus, capacity for strong hydrogen bonding of the quinoline ring N atom and hydrophobic interactions of 1 & 2 are probably the two most important features appear to be responsible for the documented anti-COVID-19 activity [23, 24, 35]. MEP profiles of the compounds are clearly consistent with the observation (Fig. 1). In addition, since the compounds contain aromatic rings, their capacities for both pi-pi stacking and cation-pi interactions as well as pi-pi stacking interactions with the target structure cannot be ruled out. Possibility of such interactions was suggested in the reported interactions of the crystallographic structure of the inhibitor bound COVID-19 main protease (MPro) [28, 36].

Furthermore, a similarity search from literature [38–40] was carried based on MEP profiles of compounds 1 (CQ) and 2 (HCQ), which led us to identify and shortlist

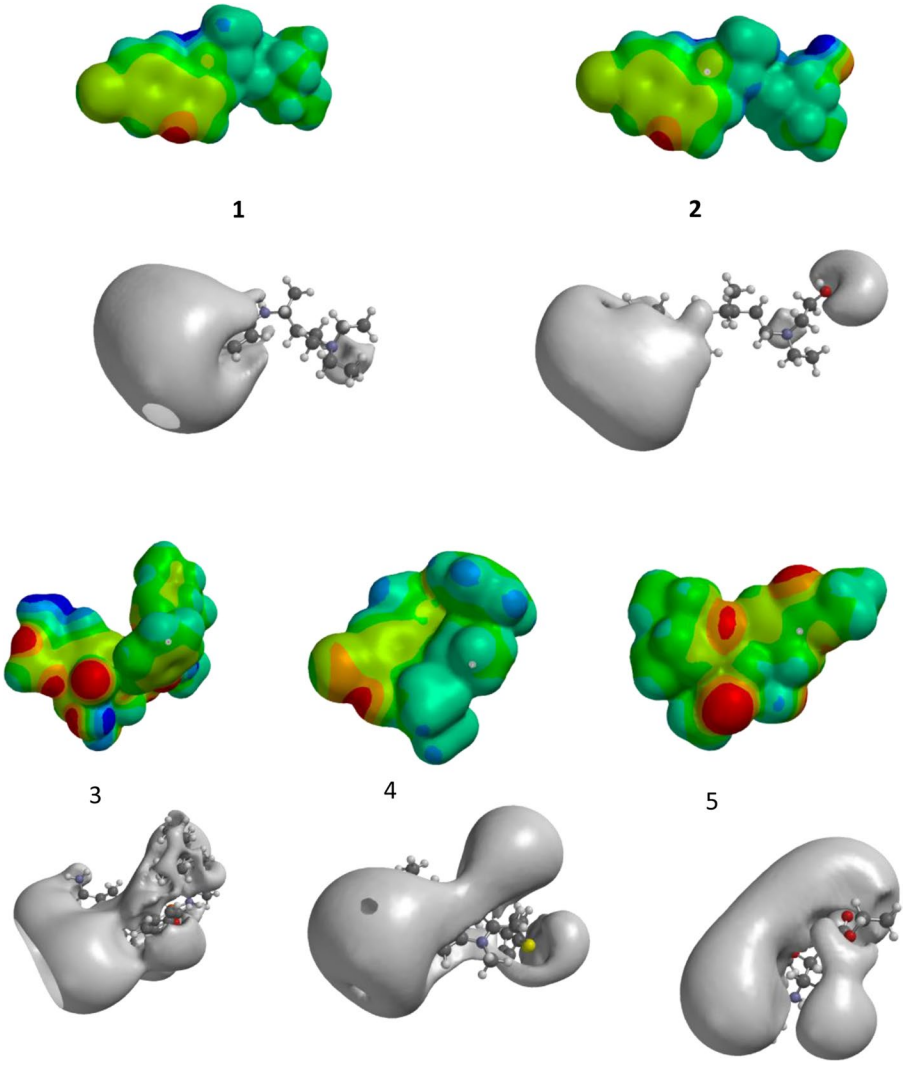

Fig. 1 MEP profiles onto van der Waals surface (upper rows) and beyond van der Waals surface at -20.0 kJ/mol (lower rows)

seven compounds. The identified compounds are shown in Chart II. The identified compounds are mostly antimalarial aminoquinolines and isoquines s including a few with reported antiviral activity against dengue and Zika viruses [37–39]. Drug-likeness properties of Chart II compounds are favorable as per the Lipinsky's rule [30]. MEP profiles of the compounds are shown in Fig. 2 (upper rows). The most negative MEP (deepest red) color locations of all the compounds are found by the quinoline nitrogen atoms (Fig. 2, upper rows) indicating the importance of H-BA capacity of quinoline nitrogen atom towards anti-COVID-19 activity. Additionally, a few other atoms of the aminoquinoline derivatives too were found to have strong negative MEP

regions (red color, Fig. 2, upper rows) indicating the ability for multiple H-BA interactions. However, it is important to note that even having the capacity for multiple H-BA interactions, steric factors may prevent such interactions due to the presence of bulkier groups around the H-BA capable centers in the molecules (Fig. 2, upper rows).

Next one views a large extended potential region by the quinoline nitrogen atoms of the compounds beyond the van der Waals surface (Fig. 2, lower rows). The figure (Fig. 2, lower rows) clearly indicates a powerful "suction-like" ability for the compounds. This characteristic feature further indicates the strength of H-bonding potential of the quinoline nitrogen and the ability of the target receptor to rapidly recognize it for interactions. Observation of this characteristic MEP feature of the Chart II compounds is found to be consistent with the compounds 1 (CQ) and 2 (HCQ) of

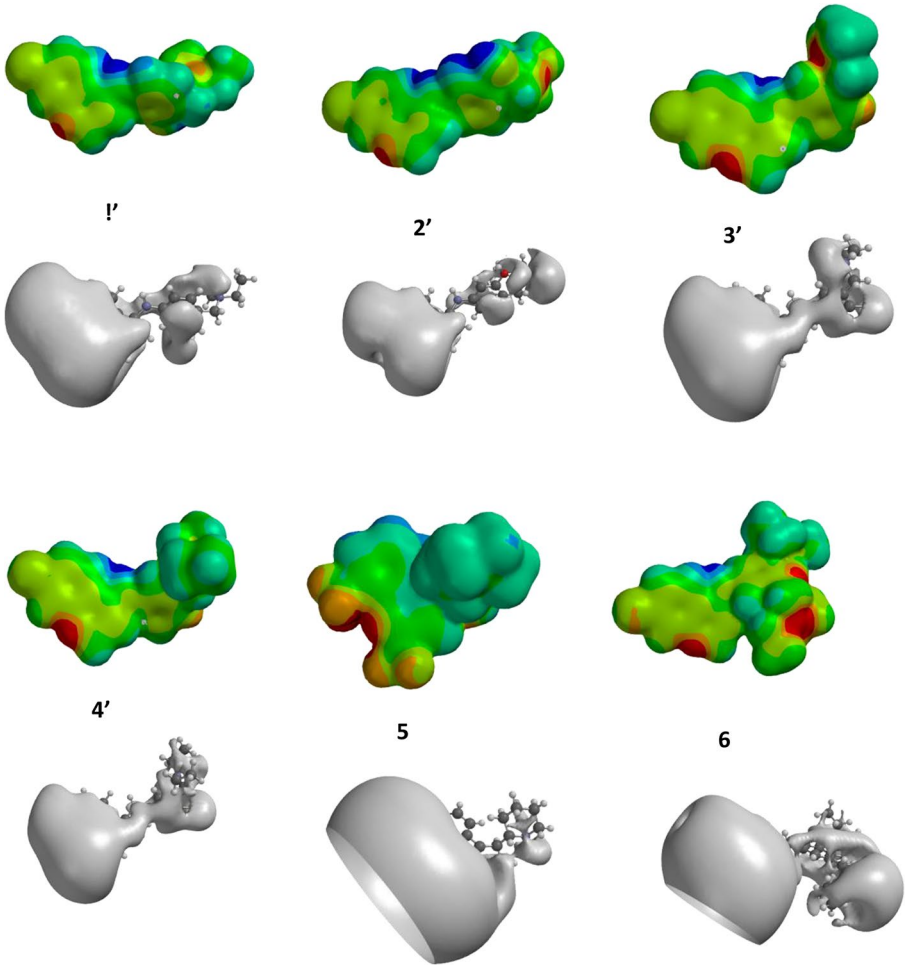

Fig. 2 MEP profiles onto van der Waals surface (upper rows) and beyond van der Waals surface at -20.0 kJ/mol (lower rows)/

Chart I indicating the potential for activity against COVID-19. Apart from H- bonding capacities, Chart II compounds should have the capacity for both hydrophobic as well as weak interactions, such as pi-pi stacking and cation-pi interactions. It is now apparent that the role of both strong hydrogen bonding and hydrophobic interactions along with capacity of weak interaction could be related for anti-COVID19 activity. The important role of quinoline ring N atom of the aminoquinolines for 1 (CQ) & 2 (HCQ) for anti-COVID-19 activity may be explained by the cellular entry mechanism of the virus in endosomes. Anti COVID-19 activity of these compounds has been reported to be facilitated by an increase of pH of endosomes, probably due to hydrogen bonding of the aminoquinoline N atoms of CQ and HCQ influencing negatively the fusion process of the virus and endosomes [36].

The interaction-pharmacophore model was further analyzed using chemical function descriptors (CFDs) of both Chart I & II compounds and by performing similarity scores of the compounds. These descriptors provide chemical characteristics of compounds and by suggesting the possible roles of H-bond acceptor (HBA) and donor (HBD), and hydrophobicity due to steric hindrance of crowded regions of a molecule in the interaction process with the target. However, it is a qualitative assessment of interaction capacity of molecule whereas MEPs can provide information about the intrinsic reactivity of the molecule more accurately. For example, the aromatic ring of benzene π system can be better addressed through cation-pi calculations from MEP profiles. Thus, the susceptibility of an aromatic ring for electrophilic substitution would mean automatic repulsion of other electron-rich regions for molecules. Although a chemist with medicinal chemistry experience would conclude the above insight simply from a glance of the structure of the molecule but for accurate assessment of strength of HBA and locations of sites, MEP calculations would be desirable. Nevertheless, similarity analysis of CFDs between the known anti-COVID-19 Chart I compounds and the identified Chart II compounds provided a rapid qualitative assessment for potential activity of the identified compounds. The CFD pharmacophore developed for aminoquinolines and isoquines was on the basis of their possible HBA, HBD and hydrophobic interactions. Interestingly, the pharmacophore developed from the MEP profiles ("interaction pharmacophore") was found to be consistent with the corresponding CFD pharmacophore.

Next for the potential of aminoquinolines and isoquine derivatives to bind to the active site of the Mpro protein, a similarity analysis of CFD pharmacophores was carried out between the two known anti-COVID-19 compounds 1 (CQ) and 2 (HCQ) and the ligand X-77 found in the x-ray crystallographic structure of Mpro protein active site [28, 36]. The analysis indicated two important observations: (1) isoquine and N-tert-butyl isoquine (compound 1' & 2', Chart II) have 90% similarity with 1(CQ) and 2 (HCQ), and (2) from the point of view of interaction capacity, the X-77 ligand was about 80% similar to compounds 1 (CQ) and 2 (HCQ). Therefore, it is reasonable to comment that compounds 1' (isoquine) and 2' (N-tert-butyl isoquine) of Chart II have high probability for anti COVID-19 activity.

Next, in order to validate of the pharmacophore, a structure-based analysis was performed. It is well documented that for drug targets of coronaviruses, the most attractive target was the main protease (Mpro, also known as 3CLpro) due its essential role in processing the polyproteins and their translational role in the viral RNA

[35]. The x-ray crystallographic structure of COVID-19 (SARS-CoV-2) Mpro had been reported with both a ligand and without a ligand [28, 36]. In this study, the target structure analyzed was 3-chymotrypsin-like protease (3CL-protease) structure as this enzyme is implicated as the main protease involved in the cleavage of polyproteins into replication-related proteins [36]. The 3CL-protease crystallographic structure (PDB code: 6W63) was deposited recently in the Protein Data Bank [28, 36]. The crystallographic protein structure reported was with a bound ligand, interaction ability of which is also found to be consistent with our developed "interaction-pharmacophore model". Briefly, analysis of the co-crystallized X77 ligand at the binding site of the 3CL-protease, Mpro structure revealed several important observations which may be summarized by five hydrogen-bonding interactions: (a) H-bond connecting the amidic NH and carbonyl of Asn142 via bridging with water molecule, (b) H-bond between the amidic carbonyl with NH of Glu166, (c) H-bond between the carbonyl oxygen with NH of Gly143, (d) imidazole N with Thr26 via two bridgings with water molecules, and (e) the H-bond interaction connecting the second imidazole N with NH of His41. Apart from these five H-bond interactions, two π- π stacking interactions are observed: (a) between the benzene ring of the inhibitor X77 and the imidazole ring of His41, and (b) π- π stacking between the pyridine ring of the inhibitor sandwiched between the benzene ring of Phe140 and the imidazole ring of His172. In addition, the tert-butyl group of X77 was found to be projected towards the Met165 and Cys44 indicating the possibility a mutual hydrophobic interaction where the inhibitor was anchored in the binding cervices of COVID-19 main protease (M^{pro}) (Fig. 3). Similar to these observed interactions of X-77 inhibitor towards anti-COVID-19 activity, compounds 1' (isoquine) and 2' (N-tert-butyl isoquine) of Chart II too have capabilities for multiple H-bond acceptor (HBA) (at least 3 or 4), at least one H-bond donor (HBD), ring aromaticity for π- π stacking, and at least one hydrophobic (Hbic) interactions [41–43]. Like the ligand, X77's tert-butyl group, the tert-

Fig. 3 3CL main protease structure (pdb: 6W63) with the ligand X77

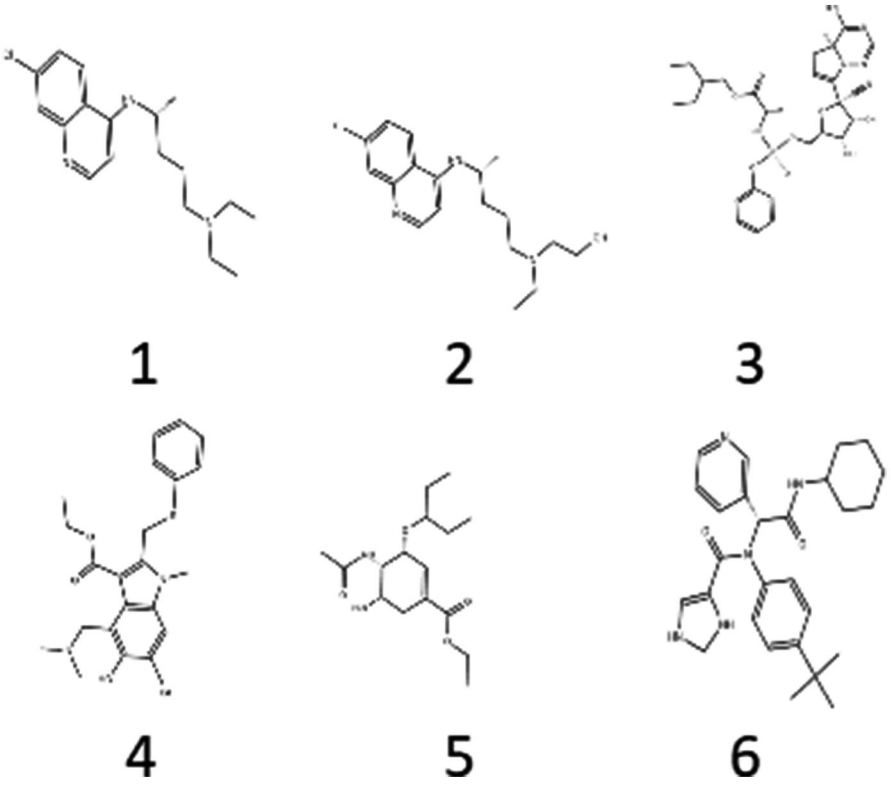

Chart I compounds: **1** (CQ, Chloroquine); **2** (HCQ, Hydroxychloroquine); **3** (Remdesivir); **4** (Arbidol); **5** (Oseltamivir); **6** (X-77 ligand inhibitor of COVID-19 main protease (Mpro) the 3CL-protease (PDB code: 6W63).

butyl group of isoquine and other aminoquinolines derivatives too can have multiple hydrogen-bond interactions in the active site, π- π stacking interactions and hydrophobic interactions within the binding pocket of COVID-19 main protease (Mpro). Similar to the hydrophobic interactions within the binding pocket of COVID-19 main protease (Mpro) site for X-77, isoquine and other aminoquinolines derivatives too can have the ability for hydrophobic interactions with Met165 and Cys44 as reported [40–42]. Thus, the "interaction pharmacophore" model developed in the study have the potential for capturing true positive hits against COVID-19 along with selectivity. Ligand interaction with the target protein plays a key role in structure-based virtual screening using pharmacophore models which are well documented as an alternative to the traditional high throughput and small molecule virtual screening approaches [41].

In order to validate the potential of our identified compounds for COVID-19 activity, we selected randomly three related diverse compounds, two aminoquinolines quinacrine (QC) & mefloquine (MQ) and an isoquine analog, N-tert-butyl isoquine for experimental testing. Plaque assays in vero cells was performed at various concentrations of the three compounds to see the effect on virus life cycle. The cell line

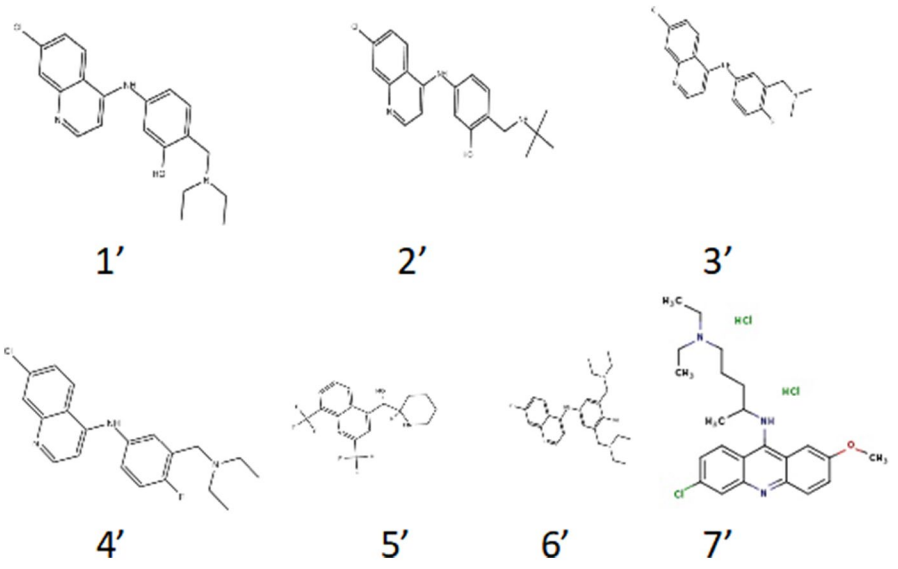

Chart II compounds: **1'** (Isoquine); **2'** (N-tert-butyl isoquine, GSK369796); **3'** (FAQ (N-Me_2); **4'** (FAQ (N-Et_2)); **5'** (Mefloquine); **6'** (Cycloquine); **7'** (Quinacrine).

used here was specifically designed to study such viral infections as well as for development of novel therapeutics targeting the virus. The results show that the IC-50 values correspond to the order: N-tert-butyl isoquine < quinacrine (QC) < mefloquine (MQ). (IC-50 is 50% inhibitory concentration required for 50% inhibition of replication of the virus with respect to the virus control). Another measurement using the CC-50 of the compounds was performed. The results also show similar order of antiviral activity with the cytotoxic concentration meaning 50% reduction of cytotoxicity in cell viability compared to controls without treatment. Furthermore, we have determined the therapeutic index (TI) of the compounds by dividing the CC-50 values of each compound by their respective IC-50 values. It is a quantitative measurement for safety of a drug. Thus, TI is the amount of a drug that is responsible for causing toxicity to a drug. Higher the value of TI, less toxic is the drug because a higher dose of a drug would be necessary to reach the toxic threshold compared to the therapeutic effect of it. The TI values of the above three compounds correspond to the following order: N-tert-butyl isoquine > quinacrine (QC) > mefloquine (MQ).

Now, experimental evidence on both drugs, compounds 1 (CQ) and 2 (HCQ) of Chart I that were used for COVID-19 treatments have shown EC_{90} values around 6.90 mM against COVID-19 in Vero E6 cells [35, 43]. Mechanism of action for both CQ and HCQ are believed to occur by inhibition of lysosomal activity due to increase of pH in the intracellular APCs (antigen-presenting cells), pDCs (plasmacytoid dendritic cells) and B cells [39].

Being similar in structure and interaction pharmacophore profiles with CQ and HCQ, our model identified aminoquinoline and isoquine derivatives are likely to have anti-COVID19 activity. Additionally, isoquine derivatives have special advantage, particularly the N-tert-butyl isoquines as these compounds are less likely to

be toxic compared to 1 (CQ) and 2 (HCQ) of Chart I. This is because isoquine analogs like N-tert-butyl isoquines (compounds 1' and 2') of Chart II cannot form quinoneimine, the toxic metabolites via cytochrome due to the hydroxyl group in the Mannich side chain in its structure. Due to the hydroxyl group substituent in the structure, N-tert-butyl isoquines not only retains bonding interactions with the aromatic hydroxyl group but also is prevented from oxidation to toxic metabolites. Furthermore, N-tert-butyl isoquine (compounds 2') of Chart II is reported to have better pharmacodynamic & pharmacokinetic properties, oral bioavailability, low toxicity in vitro studies, and reasonable safety profile than other isoquine analogs and aminoquinolines in pre-clinical studies [37, 38].

4 Concluding remarks and future scope

This review provides a range of theoretical approaches attempted in recent years for discovery of COVID-19 therapeutics. Although no successful COVID-19 drug had been achieved so far by using any of these methods, different studies presented here could be milestones for future theoretical studies to achieve the goal. The theoretical study from the author's lab demonstrated a rational approach for discovery of compounds having the potential for activity against COVID19 and validated the identified compounds with experimental antiviral activity. By using quantum chemical and semi-empirical calculations for developing "interaction pharmacophore" model and focusing particularly on molecular electrostatic potentials (MEPs), it was possible to identify new compounds having the potential for activity against COVID-19. Additional theoretical analyses supported consistency of interactions with the inhibitor bound x-ray crystallographic structure at the active site of Mpro, the main COVID-19 protein. The author's model based identified compounds and their experimental validation for antiviral activity indicate the potential for activity against COVID19, thus strengthen the usefulness of theoretical approaches towards discovery of COVID-19 therapeutics. However, despite isoquine and its derivatives are promising and known to have less toxicity, further study would be necessary to make them successful therapeutics. Nonetheless, the study not only signifies therapeutic importance of the identified compounds but also demonstrates the utility of computational chemistry towards design and discovery of potential COVID-19 drugs.

However, despite availability of preventive measures from vaccines and two drugs for COVID-19 treatments there are quite a few challenges remained to be overcome for new discovery. The major challenges are for patients who are immunocompromised or have vaccine immunity. An important emerging issue is the nature of prolonged COVID-19, known as long-COVID suffering patients,. The symptoms are not only found in hospitalized patients but also reported for people suffering from mild to moderate COVID-19 infection. Long-COVID is reported to be more severe than other post-viral syndromes since patients admitted in hospitals with diabetes and cardiovascular problems have significantly higher rates of death compared to patients admitted with influenza [44]. Long-COVID also shows neurological and mental health disorders, fatigue, and coagulation disorders [44]. Pathogenic-profiles of gut–lungs microbiome interactions were also reported to affect the host immunity

in case of long-COVID patients [10]. Since the mechanism of long-COVID is still not well understood, discovery of new COVID-19 drugs should consider the above issues for clinical studies before a potential COVID drug be promoted. However, rapid discovery for small molecule antivirals will not only advance the development of better COVID-19 therapies but would help to face other challenges from future pathogens and pandemics. Furthermore, due to the shortcomings of presently available vaccines to prevent some variants of COVID-19, direct acting antiviral drugs could be an additional necessity. Thus, future efforts should be more coordinated with antivirals along with complementary synergic support from newer vaccines. Small molecule discovery should engage in the functional site of COVID-19 protein to disrupt its cellular function. However, for ideal COVID-19 treatments, the drug should have a good safety profile to prevent clinical deteriorations and hospitalization and finally should be less expensive and effective for a large population.

Acknowledgements Audience of Eighth Indo-US workshop, September 2022 for valuable suggestions in writing the manuscript.

Author contributions Author wrote the full manuscript, performed all computational works, validated the model with experimental data from a previously published work by citing its reference.

Funding None.

Data availability Published literature based data.

Declarations

Ethical approval Not applicable.

Competing interests The authors declare no competing interests.

References

1. F. Wu, S. Zhao, B. Yu, Y.M. Chen, W. Wang, Z.G. Song, Y. Hu, Z.W. Tao, J.H. Tian, Y.Y. Pei, M.L. Yuan, Y.L. Zhang, F.H. Dai, Y. Liu, Q.M. Wang, J.J. Zheng, L. Xu, L.E.C. Holmes, Y.Z. Zhang Nat., **579** (7798): 580 (7803) 265–269, PMID: 32296181; PMCID: PMC7608129.
2. (a) WHO Coronavirus (COVID-19) Dashboard, accessed on 10 July (2023); (b) WHO from 5 January 2020–14 April 2024. Covid-19 dashboard accessed on 26 April (2024)
3. Coronavirus Disease, (COVID-19): Vaccines (WHO, accessed 15 December 2022); https://go.nature.com/40jSwuN'
4. S.S. Toussi, J.L. Hammond, B.S. Gerstenberger, A.S. Anderson, Microbiol. (Nature). **8**, 771 (2023)
5. (a) Coronavirus (COVID-19) Update: FDA Authorizes Monoclonal Antibodies for Treatment of COVID-19 (US FDA, 21 November 2020); https://go.nature.com/3JMqFME; (b) J.C. Almagro, G. Mellado-Sanchez, M. Pedraza-Escalona, S.M. Perez-Tapia, Int. J. Mol. Sci. 23, 9763 (2022); (c) COVID-19 Monoclonal Antibodies (Centers for Medicare & Medicaid Services, accessed 21 February 2023); https://www.cms.gov/monoclonal
6. L. Bull-Otterson, E.B. Gray, D.S. Budnitz, H.M. Strosnider, L.Z. Schieber, J. Courtney, M.C. García, J.T. Brooks, W.R. Mac Kenzie, A.V. Gundlapalli, *Morbidity and Mortality Weekly Report, September 4, 2020 /* Vol. 69 / No. 35 US Department of Health and Human Services/Centers for Disease Control and Prevention. 1210–1215

7. FDA NEWS RELEASE, Coronavirus (COVID-19) update: FDA authorizes first oral antiviral for treatment of COVID-19, December **22**, (2021)
8. S. Drożdżal, J. Rosikb, K. Lechowiczc, F. Machajb, B. Szostakb, J. Przybycin, S. ́skia, K. Lorzadehd, S. Kotfisc, M.J. Ghavamie, Łosj, Drug Resist. Updates. **59**, 100794 (2021). https://doi.org/10.1016/j.drup.2021.100794
9. M. Mahoney, V.C. Damalanka, M.A. Tartell, D.H. Chung, A.L. Lourencọ, D. Pwee, A.E. MayerBridwell, M. Hoffmann, J. Voss, P. Karmakar, N.P. Azouz, A.M. Klingler, P.W. Rothlauf, C.E. Thompson, M. Lee, L. Klampfer, C.L. Stallings, M.E. Rothenberg, S. Pöhlmann, S.P.J. Whelan, A.J. O'Donoghue, C.S. Craik, J.W. AJanetka, J.W.A, Proc. Natl. Acad. Sci. U. S. A. 118, No. e2108728118 (2021)
10. S. Nandi, S. Ahmed, A. Saxena, A.K. Saxena, Exploring the pathoprofiles of SARS-COV-2 Infected Human gut–lungs Microbiome Crosstalks, in *Probiotics, Prebiotics, Synbiotics, and Postbiotics*, ed. by V. Kothari, P. Kumar, S. Ray (Springer, Singapore, 2023). https://doi.org/10.1007/978-981-99-1463-0_12
11. P.C. Robinsona, D.F.L. Liewc, H.L. Tannera, J.R. Graingerf, R.A. Dwekg, R.B. Reislerh, L. Steinmani, M. Feldmannk, L.P. Hol, T. Hussellf, P. Mossm, D. Richardson, N. Zitzmanng, Proc. Natl. Acad. Sci. U.S.A., 119, e2119893119, 1–10, (2022). https://doi.org/10.1073/pnas.2119893119
12. M.C.L. Teixeira, J.T.S. Coimbra, M.J. Ramos, P.A. Fernandes, J. Chem. Info Model. **62**(10), 2510–2521 (2022). https://doi.org/10.1021/acs.jcim.1c01561
13. C. Bai, A. Warshel, J. Phy Chem, B, 124 (28), 5907–5912 (2020) https://doi.org/10.1021/acs.jpcb.0c04317
14. C.A. Ramos-Guzmán, J.L. Velázquez-Libera, J.J. Ruiz-Pernía, I. Tuñón, J. Chem. Theory Comput. **18**(6), 4005–4013 (2022). https://doi.org/10.1021/acs.jctc.2c00294
15. Y. Li, L. Cao, G. Li, F. Cong, Y. Li, J. Sun, Y. Luo, G. Chen, G. Li, P. Wang, F. Xing, Y. Ji, J. Zhao, Y. Zhang, D. Guo, X. Zhang, J. Med. Chem. **65**(4), 2785–2793 (2022). https://doi.org/10.1021/acs.jmedchem.0c01929
16. T. Xu, M. Xu, W. Zhu, C.Z. Chen, Q. Zhang, W. Zheng, R. Huang, J. Med. Chem. **65**(6), 4590–4599 (2022). https://doi.org/10.1021/acs.jmedchem.1c01372
17. T.R. Malla, L. Brewitz, D.G. Muntean, H. Aslam, C.D. Owen, E. Salah, A. Tumber, P. Lukacik, C. Strain-Damerell, H. Mikolajek, M.A. Walsh, C J. Schofield J. Med. Chem. **65**(11), 7682–7696 (2022). https://doi.org/10.1021/acs.jmedchem.1c02214
18. J.M. Sasso, B.J.B. Ambrose, R. Tenchov, R.S. Datta, M.T. Basel, R.K. DeLong, Q.A. Zhou, J. Med. Chem. **65**(10), 6975–7015 (2022). https://doi.org/10.1021/acs.jmedchem.2c00024
19. I. Vorobyov, I. Kim, Z.T. Chu, A. Warshel, Proteins: Struct Funct Genet, 84, 92 – 117 (2016)
20. R. Dey, A. Samadder, S. Nandi, Curr Top Med Chem, 22(29), 2410–2434, (2022), doi: 10.2174/1568026623666221130142517. PMID: 36453483
21. S. Nandi, B.S. Nayak, M.K. Khede, A.K. Saxena, Curr Top Med Chem, 22(32), 2660–2694 (2022). https://doi.org/10.2174/1568026623666221130142517. PMID: 36453483
22. S.C. Basak, S. Majumdar, M. Vracko, A. Nandy, A.K. Bhattacharjee, Curr. Comput-Aided Drug Des. **16**, 1–3 (2020)
23. A.K. Bhattacharjee, Abstract 8th Indo-US workshop on Mathematical Chemistry. September 13–17, (2022)
24. A.K. Bhattacharjee, J. Med. Chem. Drug Des. **1–**, 102 (2021)
25. G. Li, E. De Clerck, Nat. Rev. Drug Discovery. **19**, 149–150 (2020). https://doi.org/10.1038/d41573-020-00016-0
26. Q. Liu, X.X. Fang, T. Lu, X. Chen, U. Chung, K. Wang, D. Li, X. Dai, Q. Zhu, F. Xu, L. Shen, B. Wang, L. Yao, P. Peng, The effect of Arbidol Hydrochloride on reducing mortality of Covid-19 patients: a retrospective study of real world data from three hospitals in Wuhan. https://doi.org/10.1101/2020.04.11.20056523
27. A. Shannar, R. Peter, P.J. Chen, S. Li, R. Hudikar, X. Liu, Z. Liu, G.J. Poini, L. Amorosa, L. Brunett, A.N. Kong, Curr. Pharmacol. Rep. **11**, 1–15 (2020). https://doi.org/10.1007/s40495-020-00216-7
28. http://www.rcsborg/structure/6W63
29. Spartan'18 Software from Wavefunction, Inc, (2020)
30. , ed. by C.A. Lipinsky, D.D. Today Technologies, (2004). https://doi.org/10.1016/j.ddtec.2004.11.007 (b) G.M. Rishton Review. Drug Discov Today, 8, 86–96 (2003)
31. M.P. Gleeson, J Med Chem, 51(4), 817 – 34 (2008). https://doi.org/10.1021/jm701122q. Epub 2008 Jan 31.PMID: 18232648
32. J. Tomasi, B. Mennucci, R. Cammi, Chem. Rev. **105**, 2999–3093 (2005)

33. T. Nusser, T. Balogh, G. Naray-Szabo, J. Mol. Struct. **297**, 127–132 (1993)
34. A.R. Leach, *Molecular Modelling, Principles and Applications* (A.W. Longman Ltd.,, 1998). Essex CM20 2JE, England
35. D. Zhou, S.M. Dai, Q. Tong, J. Antimicrob. Chemother. **75**, 1667–1670 (2020). https://doi.org/10.1093/jac/dkaa114
36. Z. Jin, X. Du, Y. Xu, Y. Deng, M. Liu, Y. Zhao, B. Zhang, X. Li, L. Zhang, C. Peng, bioRxiv, RCSB Protein Data Bank (2020)
37. P.M. O'Neill, V.E. Barton, S.A. Ward, J. Chadwick, 4-aminoquinolines: chloroquine, amodiaquine and next-generation analogues. In:, H.M. Staines, S. Krishna Treatment and Prevention of Malaria. (, P.M. O'Neill, A. Mukhtar, P.A. Stocks, L.E. Randle, S. Hindley, S.A. Ward, R.C. Storr, J.F. Bickley, I.A. O'Neil, J.L. Maggs, R.H. Hughes, P.A. Winstanley, P.G. Bray, B.K. Park (eds.), J Med Chem 46, 4933–4945 (2003)
38. A. Balasubramanian, T. Teramoto, A.A. Kulkarni, A.K.Bhattacharjee, R. Padmanabhan, Antivir Res. **137**, 141–150 (2017)
39. S. Boonyasuppayakorn, E.D. Reichert, M. Manzano, K. Nagarajan, R. Padmanabhan, Antivir Res. **106**, 125–134 (2014)
40. M. Arooj, S. Sakkiah, S. Kim, V. Arulalapperumal, K.W. Lee, PLoS One, **8**, (4) (2013)
41. A. Gaurav, V. Gautam, S. Pereira, J. Alvarez-Leite, F. Vetri, M. Choudhury, D. Pelligrino, P. Sundivakkam, K. Radhakrishnan, A. Krieger, J. Recept Ligand Channel Res. **7**, 27–38 (2014)
42. M.P. Sanders, R. McGuire, L. Roumen, I.J. de Esch, J. de Vlieg, J.P. Klomp, C. de Graaf, Med. Chem. Comm. **3**(1), 28–38 (2012)
43. M.J. Vincent, E. Bergeron, S. Benjannet et al., Virol. J. **2**, 69 (2005)
44. C. Philip, D.F.L. Robinsona, H.L. Liewc, J.R. Tannera, D.R.A. Grainge, R.B. Reislerh, L. Steinmani, M. Feldmannk, H. Ling-Pei, T. Hussellf, P. Mossm, D. Richardsn, N. Zitzmanng, Proc. Natl. Acad. Sci. **119**, 15, e2119893119 (2022). https://doi.org/10.1073/pnas.2119893119